Int. J. Heat Mass Transfer. Vol. 21, pp. 549–556

0017-9310/78/0501-0549 $02.00/0

HIGHER ORDER APPROXIMATIONS TO THE NATURAL CONVECTION FLOW OVER A UNIFORM FLUX VERTICAL SURFACE

R. L. MAHAJAN† and B. GEBHART
Department of Mechanical Engineering, State University of New York at Buffalo, Buffalo, NY 14214, U.S.A.

(*Received* 21 *March* 1977 *and in revised form* 19 *September* 1977)

Abstract—Perturbation analysis of higher order boundary-layer effects for convection flow over a semi-infinite vertical uniform flux surface is presented. Using asymptotic matching technique, three term inner and outer expansions have been obtained. Eigenvalues and their eigenfunctions associated with the inner expansions have also been investigated and it has been shown that their contribution to these three term expansions is identically zero. The numerical results for $Pr = 0.733$ and 6.7 show that the higher order corrections to the local temperature difference and the local skin friction are negative but are positive to the local Nusselt number. Considerations of global momentum and buoyancy indicate an indeterminacy of $O(1)$ in the expression for total drag.

NOMENCLATURE

- BL, boundary layer;
- c_p, specific heat of the fluid;
- D, total drag on plate between leading edge and local x (per side per unit width);
- Gr_x, local Grashof number, $\frac{g\beta_t \Delta T x^3}{\nu^2}$;
- Gr_x^*, local flux Grashof number, $\frac{g\beta_t q_w x^4}{k\nu^2}$;
- G, modified Grashof number, $4\left(\frac{Gr_x}{4}\right)^{1/4}$;
- G^*, modified flux Grashof number, $5\left(\frac{Gr_x^*}{5}\right)^{1/5}$;
- g, gravitational acceleration;
- h, heat-transfer coefficient;
- k, thermal conductivity;
- Nu_x, local Nusselt number, hx/k;
- p, pressure;
- Pr, Prandtl number, $\frac{\mu c_p}{k}$;
- q_w, local heat flux from plate;
- Q, total heat-transfer rate from plate between leading edge and local x (per side and per unit width);
- r, polar radial coordinate;
- t, temperature;
- t_∞, temperature of ambient fluid;
- T, $= (t - t_\infty/\Delta T)$;
- u, x component of velocity;
- v, y component of velocity;
- x, vertical coordinate;
- X, $1/5\left(\frac{k\nu^2}{g\beta_t q_w}\right)^{1/4}$;
- y, horizontal coordinate.

Greek symbols

- β_t, coefficient of thermal expansion;
- δ, characteristic boundary-layer thickness;
- ΔT, characteristic temperature difference across the boundary layer;
- ε, perturbation parameter, $\equiv \delta/x = 5/G^*$;
- η, $\equiv y/\delta$;
- θ, angular coordinate measured from plate;
- μ, dynamic viscosity;
- ν, the kinematic viscosity;
- ρ, density of fluid;
- Ψ, stream function;
- ω, resultant flow velocity.

† Present address: Engineering Research Center, Western Electric, P.O. Box 900, Princeton, NJ 08540, U.S.A.

1. INTRODUCTION

THE ANALYTICAL studies of higher order boundary-layer effects for natural convection flow around a semi-infinite vertical isothermal surface are many [1–4]. In all these studies, the classical boundary-layer solution due to Pohlhausen [5] is taken as the leading term in the asymptotic expansion for large Grashof number of the full solution of the problem, with the expansion parameter as $1/G$.

Yang and Jerger [1] obtained first order corrections both for the semi-infinite and finite vertical plate. Their calculated correction to the Nusselt number obtained from the boundary-layer theory is negative. This, as pointed out by Gebhart in a comment following their paper, is at variance with the experimental data at low Grashof numbers, which indicates values of Nusselt number higher than predicted by boundary-layer theory. This matter was later taken up by Hieber [3], who on the basis of global energy considerations showed that the boundary-layer expansion gives rise to an additional term which results in a net positive first order correction to the total heat-transfer rate. He also pointed out an error due to improper matching in the second order correction obtained earlier by Kadambi [2] and, in addition, obtained the first three eigenvalues and the corresponding eigenfunctions appearing in the boundary-layer expansion. The multiplicative constants associated with these eigenfunctions are, however, indeterminate. The analysis of Riley and Drake [4] is similar to that of Kadambi [2] and has the same improper matching conditions in the second order equations.

All of the above studies are for a surface with uniform temperature. However, an important practical and experimental circumstance in many natural convection flows is that generated adjacent to a surface dissipating heat uniformly. There is no prior investigation of the higher order effects for this condition. In the present paper, we obtain perturbation solutions, in terms of perturbation parameter, $\varepsilon = 5/G^*$. Matched asymptotic expansions are used to construct inner and outer expansions for velocity, temperature and pressure. The first three terms of the series are calculated for both air ($Pr = 0.733$) and water ($Pr = 6.7$). The eigenfunctions associated with the boundary-layer expansions are considered and it is shown that their contribution to the solution is identically zero.

2. ASYMPTOTIC EXPANSIONS

The present problem is formulated on the basis of a semi-infinite vertical surface with the origin at the leading edge. The x axis is vertically upward and y is perpendicular to the surface. Heat is dissipated uniformly at the surface. Employing the Boussinesq approximation, neglecting the viscous dissipation and the pressure terms in the energy equation, the governing equations are:

$$\frac{\partial u}{\partial x}+\frac{\partial v}{\partial y}=0 \tag{1}$$

$$\left(u\frac{\partial}{\partial x}+v\frac{\partial}{\partial y}\right)u = \nu\left(\frac{\partial^2}{\partial x^2}+\frac{\partial^2}{\partial y^2}\right)u+g\beta_t(t-t_\infty)-\frac{1}{\rho}\frac{\partial p}{\partial x} \tag{2}$$

$$\left(u\frac{\partial}{\partial x}+v\frac{\partial}{\partial y}\right)v = \nu\left(\frac{\partial^2}{\partial x^2}+\frac{\partial^2}{\partial y^2}\right)v-\frac{1}{\rho}\frac{\partial p}{\partial y} \tag{3}$$

$$\left(u\frac{\partial}{\partial x}+v\frac{\partial}{\partial y}\right)t = \frac{\nu}{Pr}\left(\frac{\partial^2}{\partial x^2}+\frac{\partial^2}{\partial y^2}\right)t \tag{4}$$

subject to boundary conditions:

$$u=0=v,\ \frac{\partial t}{\partial y}=-\frac{q_w}{k}\ \text{at}\ y=0,\ x\geqslant 0 \tag{5}$$

$$\frac{\partial u}{\partial y}=0=v,\ \frac{\partial t}{\partial y}=0\ \text{at}\ y=0,\ x<0 \tag{6}$$

$$u=v\sim 0,\ t\sim t_\infty,\ p\sim p_\infty\ \text{as}\ y\to\infty\ \text{and upstream.} \tag{7}$$

Analysis of equations (1)–(4) indicates that a small term of $O(1/G^*)$ multiplies the highest derivative terms, those representing diffusion of momentum and of the thermal energy. When $G^*\to\infty$ these terms disappear, and no solution can then satisfy all the boundary conditions. This is a singular perturbation situation which may be treated by the method of matched asymptotic expansion.

The appropriate inner expansions (without the eigenfunctions to be considered later) in the boundary layer, and the outer expansions, are:

inner:

$$\begin{aligned}\Psi &= \psi_0+\varepsilon\psi_1+\varepsilon^2\psi_2+\dots\\ &= U\delta f(\eta,\varepsilon)\\ &= U\delta[f_0(\eta)+\varepsilon f_1(\eta)+\varepsilon^2 f_2(\eta)+\dots]\end{aligned} \tag{8}$$

$$\begin{aligned}t-t_\infty &= \Delta T\,T(\eta,\varepsilon)\\ &= \Delta T[T_0(\eta)+\varepsilon T_1(\eta)+\varepsilon^2T_2(\eta)+\dots]\end{aligned} \tag{9}$$

$$p-p_\infty = \rho U^2P(\eta,\varepsilon)=\rho U^2[\varepsilon^2P_2(\eta)+\dots] \tag{10}$$

outer:

$$\Psi=\bar\psi_0+\bar\psi_1+\bar\psi_2+\dots \tag{11}$$

$$t-t_\infty=\bar T_0+\bar T_1+\bar T_2+\dots \tag{12}$$

$$p-p_\infty=\bar P_0+\bar P_1+\bar P_2+\dots \tag{13}$$

where $U=\nu G^{*2}/5x$, $\delta=5x/G^*$, $\Delta T=q_w\delta/k$ and $\eta=y/\delta$. The perturbation parameter, $\varepsilon=\delta/x=5/G^*$, is determined by consideration of the order of magnitude of the normal velocity component at the outer edge of the boundary layer.

2.1. *Perturbation equations*

We now define streamfunction Ψ so that $u=\Psi_y$ and $v=-\Psi_x$. The continuity equation, (1), is then automatically satisfied. From (8), the velocity components u and v are written as

$$u=U(f_0'+f_1'+\varepsilon^2f_2'+\dots) \tag{14}$$

$$-v=U[(4f_0-f_0'\eta)\varepsilon-\varepsilon^2f_1'\eta+\dots]. \tag{15}$$

Equations (2)–(4) are now evaluated in terms of variables defined in (9), (10), (14) and (15) and perturbation equations are obtained by collecting terms with like powers of ε. The following successive approximations are obtained.

Zeroth order. Collecting terms of the order ε^0, we obtain the following classical uniform flux boundary-layer equations.

$$f_0'''-3f_0'^2+4f_0f_0''+T_0=0 \tag{16}$$

$$\frac{T_0''}{Pr}+4f_0T_0'-T_0f_0'=0 \tag{17}$$

subject to boundary conditions:

$$f(0)=f'(0)=T_0(\infty)=f_0'(\infty)=T_0'(0)+1=0. \tag{18}$$

In the outer region, it can be easily shown, see for example, Kadambi [2], that $\bar\psi_0=0=\bar T_0=\bar P_0$.

First order. To obtain first order equations, it is first necessary to match the zeroth order boundary-layer solution ψ_0 to the first order outer solution $\bar{\psi}_1$. This, as shown in [1–3], leads to

$$\nabla^2\bar{\psi}_1 = 0,\ \bar{\psi}_{1(\theta=0)} = \nu A_0\left(\frac{r}{X}\right)^{4/5},\ \bar{\psi}_{1(\theta=\pi)} = 0(19)$$

where $A_0 = f_0(\infty)$ and the values of the stream function at $\theta = 0$ and $\theta = \pi$ correspond to the matching and boundary condition respectively. Solution to (19) is given by

$$\bar{\psi}_1 = -\frac{A_0\nu}{\sin\frac{4\pi}{5}}\left(\frac{r}{X}\right)^{4/5}\sin\tfrac{4}{5}(\theta-\pi). \quad (20)$$

Using Bernoulli's equation in the outer inviscid region,

$$\bar{P}_1 = -\tfrac{1}{2}\rho\omega^2 = -\tfrac{1}{2}\rho\frac{(\frac{4}{5}A_0)^2}{\sin^2\pi/5}\left(\frac{\nu}{X}\right)^2\left(\frac{X}{r}\right)^{2/5}. \quad (21)$$

Further, for the outer, isothermal region, $\bar{T}_1 \equiv 0$.

Noting that, as $\theta\to 0$, $r = x[1+O(\varepsilon^2\eta^2)]$ and $\theta = \varepsilon\eta + O(\varepsilon^3\eta^3)$, the behavior of $\bar{\psi}_1$ and $\bar{P}_1$ in the matching region is determined to be

$$\bar{\psi}_{1_{\theta\to 0}} = U\delta A_0\left[1 - \frac{4}{5}\varepsilon\eta\cot\frac{4\pi}{5} + \frac{4}{50}\varepsilon^2\eta^2 + \ldots\right] \quad (22)$$

and

$$\bar{P}_{1_{\theta\to 0}} = -\tfrac{1}{2}\frac{\rho U^2}{\sin^2\pi/5}(\tfrac{4}{5}A_0)^2\varepsilon^2[1+0(\varepsilon^2\eta^2)+\ldots]. \quad (23)$$

From the inner and outer expansions of the stream functions, equations (8) and (11), corresponding expansions for the velocity components can be derived. Matching of the two term inner expansion of the u component as $r\to\infty$, $\theta\neq 0$, with the concomitant two term outer expansion as $\theta\to 0$, gives $f_1'(\infty) = \frac{4}{5}A_0\cot\pi/5$. The first order inner problem may be written as:

$$f_1''' + 4f_1''f_0 - 2f_0'f_1' + T_1 = 0 \quad (24)$$

$$\frac{T_1''}{Pr} + 4f_0T_1' + 3f_0'T_1 - T_0f_1' = 0 \quad (25)$$

subject to boundary conditions:

$$f_1(0) = 0 = f_1'(0) = T_1(\infty) = T_1'(0),\quad f_1'(\infty) = \tfrac{4}{5}A_0\cot\pi/5 \quad (26)$$

In particular, from (24) to (26), $f_1 \sim \frac{4}{5}A_0\eta\cot\pi/5 + A_1$ where A_1 is a numerically determined constant.

Second order. Knowing the asymptotic behavior of f_1 as $\eta\to\infty$, and matching the two term inner and outer stream function, it is easily deduced that

$$\nabla^2\bar{\psi}_2 = 0,\ \bar{\psi}_{2(\theta=0)} = 5\nu A_1,\ \bar{\psi}_{2(\theta=\pi)} = 0. \quad (27)$$

The solution to (27) is

$$\bar{\psi}_2 = 5A_1\nu\left(1-\frac{\theta}{\pi}\right). \quad (28)$$

As before, Bernoulli's equation gives

$$\bar{P}_2 = -\frac{4}{5}\frac{A_1A_0}{\sin\pi/5}\left(\frac{\nu}{X}\right)^2\left(\frac{X}{r}\right)^{6/5}\rho\cos\tfrac{4}{5}(\theta-\pi). \quad (29)$$

Finally, the second order governing equations for the boundary layer region are:

$$P_2' = \frac{\eta}{25}f_0''' - \frac{2}{25}f_0'' + \frac{4}{25}\eta f_0f_0'' + \frac{\eta}{25}f_0'f_0' - \frac{16}{25}f_0f_0' \quad (30)$$

$$f_2''' + 4f_0f_2'' + 2f_0'f_2' - 4f_2f_0'' + T_2 + 2P_2 + \eta P_2' - \frac{2}{25}f_0' + \frac{\eta^2}{25}f_0''' + f_1'^2 = 0. \quad (31)$$

$$\frac{T_2''}{Pr} + 4f_0T_2' + 7f_0'T_2 + \frac{\eta^2}{25}\frac{T_0''}{Pr} + \frac{4}{25}\frac{\eta}{Pr}T_0' - \frac{4}{25Pr}T_0 + 3T_1f_1' - f_2'T_0 - 4f_2T_0' = 0 \quad (32)$$

with the boundary conditions

$$f_2(0) = f_2'(0) = T_2'(0) = T_2(\infty) = 0,\quad P_2(\infty) = -\frac{8}{25}\frac{A_0^2}{\sin^2\pi/5} \quad (33)$$

The boundary condition on P_2 is obtained from matching considerations and the use of equation (23).

3. EIGENFUNCTIONS

The correct form of the series expansion in (8) and (9) includes a combination of the eigenfunctions which identically satisfy the boundary conditions at $\eta = 0$ and $\eta = \infty$. Their existence can be investigated as follows.

Let "λ_n" be the eigenvalue associated with the boundary-layer expansions (8) and (9) and $C_n\varepsilon^{\lambda_n}F_n(\eta)$ and $C_n\varepsilon^{\lambda_n}\phi_n(\eta)$ be the associated eigenfunctions, respectively. C_n is the multiplicative constant, which as pointed out by Stewartson [7], is associated with the stream function upstream. Including these terms in (8) and (9) and, substituting in (2) and (4), we get the following linear homogeneous equations in F_n and ϕ_n.

$$(-4\lambda_n+6)f_0'F_n + 4(\lambda_n-1)F_nf_0'' - 4f_0F_n'' = F_n''' + \phi_n \quad (34)$$

$$\frac{\phi_n''}{Pr} + 4f_0\phi_n' + 4F_nT_0'(1-\lambda_n) - F_n'T_0 + \phi_nf_0'(4\lambda_n-1) = 0 \quad (35)$$

with the boundary conditions

$$F_n(0) = F_n'(0) = F_n'(\infty) = \phi_n'(0) = \phi_n(\infty) = 0. \quad (36)$$

Non-trivial solutions of these equations exist for only particular values of λ_n. The smallest such eigenvalue of λ_n is $\frac{5}{4}$ and the associated eigenfunctions are

$$\phi_1 = C_1(T_0 - \eta T_0') \quad (37)$$

and

$$F_1 = C_1(4f_0 - \eta f_0'). \quad (38)$$

Other eigenvalues found by numerical solution of equations (34)–(36) have values greater than 2 and hence will not appear in our expansion (8) and (9).

Constants C_n in general are indeterminate, see for example Hieber [3]. However, in the present particular circumstance, it can be shown that at least $C_1 \equiv 0$.(Convected thermal energy + heat conducted in the streamwise direction)$_{BL}$ = total heat transferred from the wall to the flow, i.e.

$$\rho c_p \int_0^\infty u(t-t_\infty)\,dy - k\int_0^\infty \frac{\partial t}{\partial x}\,dy = q_w x$$

or

$$5Prq_w x\int_0^\infty \{(f_0'+\varepsilon f_1'+\varepsilon^{5/4}C_1F_1'+\varepsilon^2 f_2')$$
$$\times (T_0+\varepsilon T_1+C_1\varepsilon^{5/4}\phi_1+\varepsilon^2 T_2)\}\,d\eta$$
$$-\varepsilon^2 x q_w\int_0^\infty \left(-T_0'\frac{\eta}{5}+\frac{T_0}{5}\right)d\eta = q_w x$$

i.e.

$$\int_0^\infty [(f_0'T_0)+\varepsilon(f_1'T_0+f_0'T_1)$$
$$+C_1\varepsilon^{5/4}(F_1'T_0+f_0'\phi_1)$$
$$+\varepsilon^2(f_0'T_2+f_1'T_1+f_2'T_0)+h.o.t]\,d\eta$$
$$=\frac{1}{5Pr}-\frac{1}{25Pr}\varepsilon^2\int_0^\infty [(T_0'\eta-T_0)+h.o.t.]\,d\eta. \tag{39}$$

Equating like powers of ε on both sides, we get

$$\varepsilon^0:\int_0^\infty f_0'T_0\,d\eta=\frac{1}{5Pr} \tag{40}$$

$$\varepsilon^1:\int_0^\infty (f_0'T_1+f_1'T_0)\,d\eta=0 \tag{41}$$

$$\varepsilon^2:\int_0^\infty \left[(f_0'T_2+f_1'T_1+f_2'T_0)+\frac{1}{25Pr}(T_0'\eta-T_0)\right]d\eta=0$$

or

$$\int_0^\infty (f_0'T_2+f_1'T_1+f_2'T_0)\,d\eta=\frac{2}{25Pr}T_0 \tag{42}$$

$$\varepsilon^{5/4}: C_1\int_0^\infty (F_1'T_0+f_0'\phi_1)\,d\eta=0$$

$$C_1\int_0^\infty \{(4f_0'-f_0'-\eta f_0'')T_0+f_0'(T_0-\eta T_0')\}\,d\eta=0$$

$$4C_1\int_0^\infty (f_0'T_0)\,d\eta - C_1\int_0^\infty \eta\frac{d}{d\eta}(f_0'T_0)\,d\eta=0$$

or

$$5C_1\int_0^\infty (f_0'T_0)\,d\eta=0. \tag{43}$$

From (40),

$$\int_0^\infty f_0'T_0\,d\eta\neq 0.$$

Therefore (43) implies that $C_1\equiv 0$. It is thus concluded that boundary layer expansions (8)–(10) are appropriate up to order ε^2. It may be noted in passing that (40)–(42) can be shown to be automatically satisfied by the solution of governing equations for T_0, T_1 and T_2, respectively.

4. NUMERICAL RESULTS AND DISCUSSION

The inner region equations derived in Section 3 were solved numerically using fourth order Runge–Kutta method. The governing equations for f_i and T_i, $i = 0$–2, were integrated from η_e to $\eta = 0$, using their asymptotic values at large η (see Mahajan [8]), missing initial values of f_i and T_i were determined. These values and other numerical data of interest for both $Pr = 0.733$ and 6.7, are summarized below:

Table 1.

	$f_i''(0)$		$T_i(0)$		A_i		η_e	$\Delta\eta$
	$Pr = 0.733$	$Pr = 6.7$	$Pr = 0.733$	$Pr = 6.7$	$Pr = 0.733$	$Pr = 6.7$	for both Pr	
$i = 0$	0.8089306	0.356332	1.4798071	0.841702	0.50750508	0.20582254	6	0.05
$i = 1$	−0.083596	−0.006691	−0.3614116	−0.082575	−1.109141	−0.5374596	12	0.05
$i = 2$	−0.4461	−0.001106	−2.3230	−0.2488	2.6414	0.14178	12	0.01

The velocity and temperature profiles associated with the above solutions are illustrated in Figs. 1–4 while the pressure distributions for both values of Prandtl number are plotted in Fig. 5.

The temperature difference across the boundary layer to three terms is given by

$$\Delta T = t_0 - t_\infty = \frac{q_w\delta}{k}[T_0(0)+\varepsilon T_1(0)+\varepsilon^2 T_2(0)] \tag{44}$$

$$=\frac{5q_w}{k}X^{4/5}x^{1/5}[T_0(0)+\varepsilon T_1(0)+\varepsilon^2 T_2(0)]$$

$$=\frac{5q_w}{k}X^{4/5}T_0(0)x^{1/5}\times\left[1+\varepsilon\frac{T_1(0)}{T_0(0)}+\varepsilon^2\frac{T_2(0)}{T_0(0)}\right] \tag{45}$$

$$=\frac{5q_w}{k}X^{4/5}T_0(0)x^{1/5}(1-0.224229\varepsilon-1.5698\varepsilon^2)\quad \text{for } Pr=0.733 \tag{46a}$$

$$=\frac{5q_w}{k}X^{4/5}T_0(0)x^{1/5}(1-0.098105\varepsilon-0.2956\varepsilon^2)\quad \text{for } Pr=6.7. \tag{46b}$$

Relation (45) shows how the boundary layer 1/5th law of surface temperature variation for uniform flux ($\Delta T \propto x^{1/5}$) is modified by the higher order corrections. In particular, for both $Pr = 0.733$ and 6.7, from (46a) and (46b), the boundary-layer theory overpredicts the value of ΔT, the effect being more pronounced for lower Prandtl number.

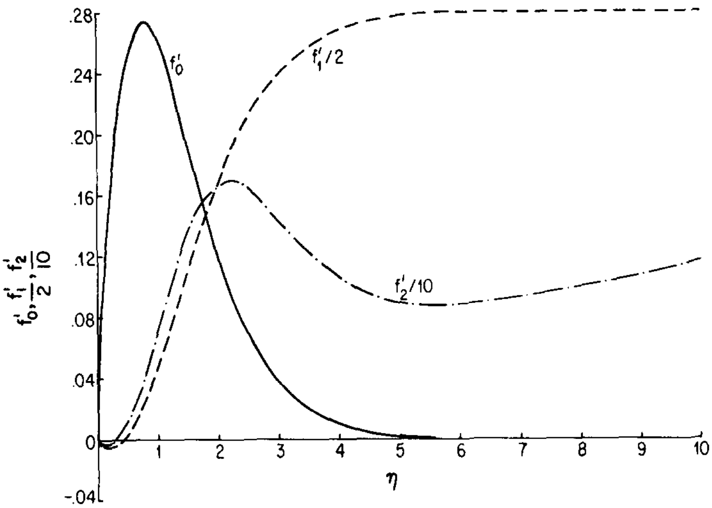

FIG. 1. Velocity function distributions for $Pr = 0.733$.

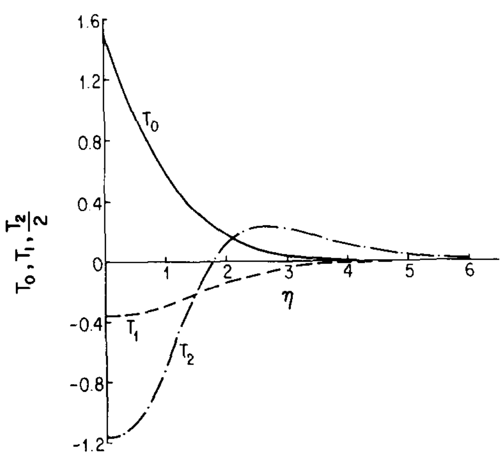

FIG. 2. Temperature function distributions for $Pr = 0.733$.

The improved local value of heat-transfer coefficient is

$$h_x = \frac{q_w}{(t_0 - t_\infty)} = \frac{k}{\varepsilon x}\left[\frac{1}{T_0(0)+\varepsilon T_1(0)+\varepsilon^2 T_2(0)}\right]$$
$$= \frac{k}{\varepsilon T_0(0) x}\left[1 - \varepsilon\frac{T_1(0)}{T_0(0)} - \varepsilon^2\left(\frac{T_2(0)}{T_0(0)} - \frac{T_1^2(0)}{T_0^2(0)}\right)\right] \tag{47}$$

so that

$$Nu_x = \frac{1}{\varepsilon T_0(0)}\left[1 - \varepsilon\frac{T_1(0)}{T_0(0)} - \varepsilon^2\left(\frac{T_2(0)}{T_0(0)} - \frac{T_1^2(0)}{T_0^2(0)}\right)\right]. \tag{48}$$

Substituting the numerical values of $T_i(0)$, we get

$$\frac{Nu_x}{Nu_{x0}} = 1 + 0.224229\varepsilon + 1.6294\varepsilon^2 \quad \text{for } Pr = 0.733 \tag{49a}$$

$$= 1 + 0.098105\varepsilon + 0.3052\varepsilon^2 \quad \text{for } Pr = 6.7 \tag{49b}$$

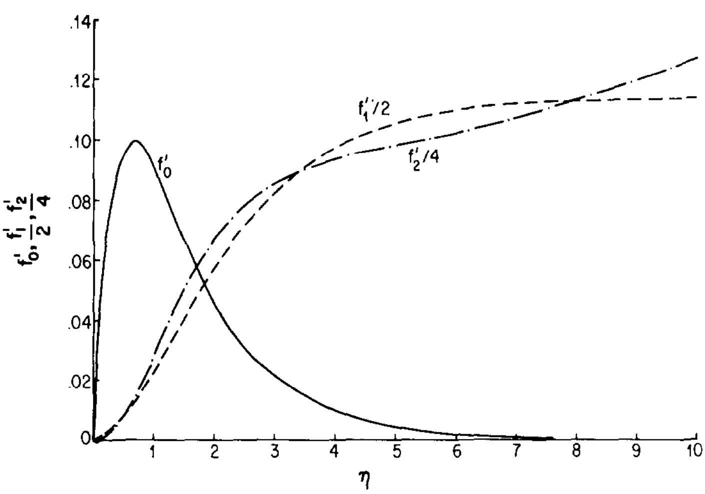

FIG. 3. Velocity function distributions for $Pr = 6.7$.

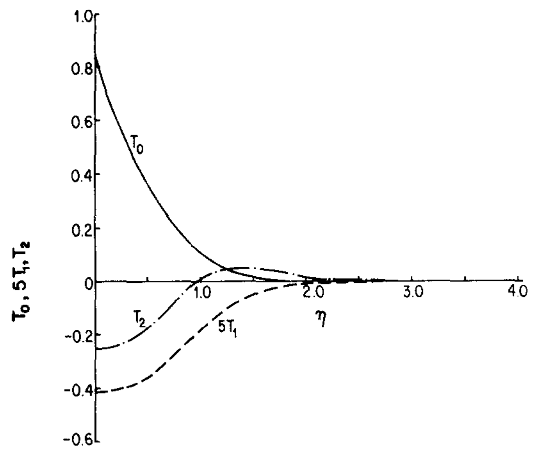

FIG. 4. Temperature function distribution for $Pr = 6.7$.

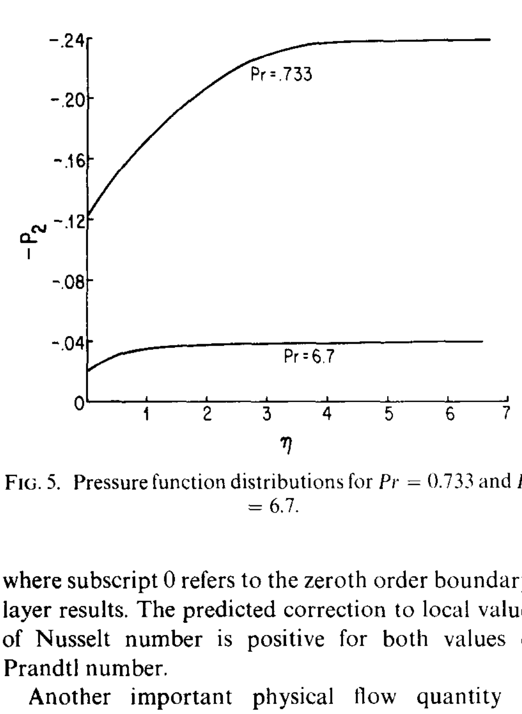

FIG. 5. Pressure function distributions for $Pr = 0.733$ and $Pr = 6.7$.

where subscript 0 refers to the zeroth order boundary-layer results. The predicted correction to local values of Nusselt number is positive for both values of Prandtl number.

Another important physical flow quantity of interest is the skin friction τ_w calculated as

$$\tau_w = \mu\left(\frac{\partial u}{\partial y}\right)_{y=0}$$

so that

$$\tau_w = \mu\frac{U}{\delta}f_0''(0)\left(1+\frac{\varepsilon f_1''(0)}{f_0''(0)}+\frac{\varepsilon^2 f_2''(0)}{f_0''(0)}+\dots\right). \quad (50)$$

The local coefficient of skin friction c_f defined as $\tau_w/(\rho U^2)$ becomes

$$c_f = \frac{5}{\varepsilon}f_0''(0)\left[1+\varepsilon\frac{f_1''(0)}{f_0''(0)}+\varepsilon^2\frac{f_2''(0)}{f_0''(0)}+\dots\right]. \quad (51)$$

In particular,

$$\frac{\tau_w}{\tau_{wo}} = 1-0.103341\varepsilon-0.5515\varepsilon^2 \quad \text{for } Pr = 0.733 \quad (52a)$$

$$= 1-0.018777\varepsilon-0.003104\varepsilon^2 \quad \text{for } Pr = 6.7. \quad (52b)$$

Note that the improved estimates of the various physical flow quantities obtained above are valid only in the region for $\varepsilon < O(1)$ i.e. $x > O(X)$. In the region of the leading edge, the functions are inapplicable. This is also seen from the singular behavior of some of the higher order terms in expressions (45)–(49) at $x = 0$. Of these, the singularities in ΔT, h_x and τ_w are non-integrable at $x = 0$ and present a difficulty in assessing the integrated values of these quantities over the plate length. In particular, it is of interest to know the total drag D and total heat-transfer rate Q, between the leading edge and local value of x. One way of obtaining these would be to evaluate the quantities

$$\int_0^x \tau_w \, dx \quad \text{and} \quad \int_0^x q_w x,$$

respectively.

As mentioned above, τ_w has a non-integrable singularity in the third term at $x = 0$ so that the drag is not calculable by this approach. An alternate procedure which obviates this difficulty is to obtain the drag from considerations of global momentum and buoyancy. This general technique was used by Imai [9] for forced flow and by Hieber [3] for the isothermal surface in natural convection. A global force balance gives the following expression for total drag D between the leading edge and local value of x

$$D = \rho\frac{U}{\delta}x\left[\tfrac{5}{7}f_0''(0)+\tfrac{5}{3}\varepsilon f_1''(0) + O(\varepsilon^{7/4})-5\varepsilon^2 f_2''(0)+\dots\right]$$

or

$$D = \frac{\nu^2\rho}{X}5^{3/4}\left[\tfrac{1}{7}\varepsilon^{-7/4}f_0''(0)+\tfrac{1}{3}\varepsilon^{-3/4}f_1''(0) + O(1)-\varepsilon^{1/4}f_2''(0)+\dots\right] \quad (53)$$

where the $O(1)$ contribution is indeterminate and is due to global buoyant force acting throughout the leading edge region. For $Pr = 0.733$ and $Pr = 6.7$, equation (53) is rewritten as,

$$\frac{D}{D_0} = 1+\tfrac{7}{3}\varepsilon\frac{f_1''(0)}{f_0''(0)}+O(\varepsilon^{7/4})-7\varepsilon^2\frac{f_2''(0)}{f_0''(0)}+\dots$$

$$= 1-0.24113\varepsilon+O(\varepsilon^{7/4})+3.8603\varepsilon^2+\dots \quad \text{for } Pr = 0.733$$

$$= 1-0.043814\varepsilon+O(\varepsilon^{7/4})+0.02173\varepsilon^2+\dots \quad \text{for } Pr = 6.7.$$

The above results indicate that the zeroth order boundary layer overpredicts the drag for both air ($Pr = 0.733$) and water ($Pr = 6.7$) as shown by the first order correction. Further, an indeterminacy of $O(1)$ occurs before the next order correction, as was also found by Hieber [3] for the isothermal case. However, there is an important difference between the two problems. For an isothermal surface, first eigenfunction was shown to make an unbounded contribution to drag D, see Hieber [3]. For the uniform flux surface, however, there is no such unbounded term because, as shown in Section 3, the contribution due to the leading eigenfunction is identically zero.

The wall heat flux q_w in the present problem is constant so that Q is simply $q_w x$. This result is in contrast to the isothermal surface condition where q_w, evaluated on the basis of perturbation solution, has a non-integrable singularity at $x = 0$ so that $Q = \int_0^x q_w \, dx$ is not determinable. Hieber [3] avoided this difficulty by determining Q from global energy considerations. It may be noted in passing that in Section 3 of [3], Q and a_2 should read

$$Q = \rho c_p \int_{BL} u(t-t_\infty)\,dy \underline{- k \int_{BL} \frac{\partial t}{\partial x}\,dy} \text{ and } a_2 = \int_0^\infty$$

$[Pr(f_0' T_2 + f_2' T_0) \underline{- \tfrac{1}{4} T_0}]\,d\eta$, respectively. The underlined terms are due to conduction in the streamwise direction and are not included in the expression in [3]. Further, it is easily shown from the governing equations for T_2 {equation (2.29) in [3]}, that $a_2 = 4/3\,T_2'(0)$. The numerical value of the corrected a_2, however, is the same as given by Hieber [3]. The above omissions are due to an oversight.

5. CONCLUDING REMARKS

It is of interest to determine the pattern of inflow to the boundary region, i.e. entrainment. Brodowicz [11] noted that this inflow may be unsteady in character and that it influences the flow in the boundary region, particularly in the region of the leading edge when the boundary region velocities are low. For various leading edge configurations, different flow patterns were observed. These are shown in Fig. 6, taken from [11]. Although not shown in the figure, the plates 2 and 3 also were found to exhibit the flow pattern changes similar to those shown for plate 1.

The entrainment velocity field, outside the boundary region, is determined in our analysis by the outer solution $\Psi = \bar{\psi}_1 + \bar{\psi}_2$ where $\bar{\psi}_1$ and $\bar{\psi}_2$ are defined in equations (20) and (28), respectively. This solution is valid everywhere in the outer inviscid region except for a small region around the leading edge where $x = O(X)$. The streamline pattern calculated from our results is similar to the symmetrical pattern shown in Fig. 6. Recall that the solution obtained here is for symmetric flow as indicated by the boundary conditions (6). The present higher order boundary-layer analysis which is valid at moderate values of G^* thus seems to correctly predict entrainment, even in the region of the leading edge where the analysis is not completely applicable. The unsteady character of the inflow and other unsymmetric flow patterns observed in [1] are outside the scope of the present analysis.

Plate	Pattern of flow	
No. 1	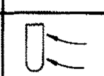	(Symmetrical)
	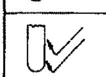	——
	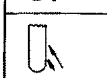	——
No. 2		(Symmetrical)
No. 3	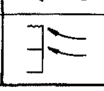	(Symmetrical)

FIG. 6. Flow pattern for plates with different leading edge configurations (from [11]).

A few other comments about the outer solution are in order. Note that the first order external pressure term $\bar{P}_1$ is independent of angular co-ordinate θ and so is the corresponding resultant velocity w. Therefore, a single hot-wire probe, traversing along a radius, may be used to map the whole outer flow fluid, to the first order.

Acknowledgements—The authors wish to acknowledge support during the period of research from the National Science Foundation under grants ENG 75-05466 and ENG 7522623 and Dr. Hieber for useful discussions with him.

REFERENCES

1. K. T. Yang and E. W. Jerger, First order perturbations of laminar free-convection boundary layers on a vertical plate, *J. Heat Transfer* **86**, 107–115 (1964).
2. V. Kadambi, Singular perturbations in free convection, *Warme- und Stoffubertragung* **2**, 99–104 (1969).
3. C. A. Hieber, Natural convection around a semi-infinite vertical plate: higher order effects, *Int. J. Heat Mass Transfer* **17**, 785–791 (1974).
4. D. S. Riley and D. G. Drake, Higher approximations to the free convection flow from a heated vertical flat plate, *Appl. Scient. Res.* **30**(3), 193–207 (1975).
5. E. Pohlauhusen, Der Wärmeaustausch zwischen festen Körpern und Flüssigkeiten mit kleiner Reibung und Kleiner Wärmeleitung, *Z. Angew. Math. Mech.* **1**, 115 (1921).
6. B. Gebhart, *Heat Transfer*, 2nd edn, p. 334. McGraw-Hill, New York (1971).
7. K. Stewartson, *The Theory of Laminar Boundary Layers in Compressible Fluids*, Section 3.5. Oxford University Press, Oxford (1964).
8. R. L. Mahajan, Higher order effects, stability and transition in vertical natural convection flows, Ph.D. Thesis, Cornell University (1977).
9. I. Imai, Second approximation to the laminar boundary-layer flow over a flat plate, *J. Aerospace Sci.* **24**, 155–156 (1958).
10. C. A. Hieber and E. J. Nash, Natural convection above a line heat source: higher-order effects and stability, *Int. J. Heat Mass Transfer* **18**, 1437–1479 (1975).
11. K. Brodowicz, An analysis of laminar free convection around isothermal vertical plate, *Int. J. Heat Mass Transfer* **11**, 201–209 (1968).

APPROXIMATIONS D'ORDRE ELEVE POUR LA CONVECTION NATURELLE SUR UNE SURFACE VERTICALE AVEC FLUX UNIFORME

Résumé—On présente une analyse de perturbation d'ordre élevé appliquée à une couche limite de convection naturelle sur une surface verticale et semi-infinie, avec flux uniforme. En utilisant une technique asymptotique, trois développements internes et externes ont été obtenus. On étudie aussi les valeurs propres et leurs fonctions propres associées aux développements internes et il est montré que leur contribution est identiquement nulle. Les résultats numériques, pour $Pr = 0,733$ et 6,7, montrent que les corrections, d'ordre élevé, de la différence de température locale et de frottement local pariétal sont négatives mais qu'elles sont positives pour le nombre de Nusselt local. Des considérations de quantité de mouvement globale et de gravité montrent une indétermination $O(1)$ dans l'expression de la trainée totale.

NÄHERUNGEN HÖHERER ORDNUNG FÜR NATÜRLICHE KONVEKTIONSSTRÖMUNG ÜBER EINE SENKRECHTE FLÄCHE

Zusammenfassung—Für eine Konvektionsströmung über eine halbunendliche, senkrechte Oberfläche mit gleichmäßiger Strömung wird eine Störungstheorie für Grenzschichteffekte höherer Ordnung angegeben. Unter Verwendung der asymptotischen Abgleichtechnik wurden dreigliedrige innere und äußere Reihenentwicklungen erreicht. Eigenwerte und ihre Eigenfunktionen wurden in Verbindung mit der inneren Reihenentwicklung ebenfalls untersucht. Es konnte gezeigt werden, daß ihr Beitrag zu dieser dreigliedrigen Reihenentwicklung Identisch O ist. Die numerischen Ergebnisse für $Pr = 0,733$ und 6,7 zeigen, daß Korrekturterme höherer Ordnung für die örtliche Temperaturdifferenz und die örtliche Wandreibung negativ sind, jedoch für die Nusselt-Zahl positiv. Betrachtungen des globalen Moments und des Auftriebs zeigen eine Unbestimmtheit von $O(1)$ im Ausdruck für den gesamten Strömungswiderstand.

ПРИБЛИЖЕНИЯ БОЛЕЕ ВЫСОКОГО ПОРЯДКА ДЛЯ РАСЧЕТА ЕСТЕСТВЕННОЙ КОНВЕКЦИИ ВДОЛЬ ВЕРТИКАЛЬНОЙ ПОВЕРХНОСТИ ПРИ УСЛОВИИ РАВНОМЕРНОГО ТЕПЛОВОГО ПОТОКА

Аннотация — Представлено исследование влияния эффектов более высокого порядка при анализе возмущений пограничного слоя для случая конвективного течения вдоль полубесконечной вертикальной поверхности при условии равномерного теплового потока. Асимптотическим методом получены трехчленные внутренние и внешние разложения. Исследованы также собственные значения и их собственные функции, связанные с внутренними разложениями, и показано, что их вклад в трехчленные разложения тождественен нулю. Численные результаты показывают, что при $Pr = 0,733$ и 6,7 поправки более высокого порядка для локальной разности температуры и локального поверхностного трения принимают отрицательное значение, а для локального числа Нуссельта — положительное. Анализ общего количества движения и подъемных сил указывает на неопределенность порядка 0(1) в выражении для полного сопротивления.